

The cataract-inducing S50P mutation in Cx50 dominantly alters the channel gating of wild-type lens connexins

Adam M. DeRosa¹, Chun-Hong Xia², Xiaohua Gong² and Thomas W. White^{1,*}

¹Department of Physiology and Biophysics and the Graduate Program in Genetics, State University of New York, Stony Brook, NY 11794, USA

²School of Optometry and Vision Science Program, University of California at Berkeley, Berkeley, CA 94720, USA

*Author for correspondence (e-mail: thomas.white@sunysb.edu)

Accepted 17 September 2007

Journal of Cell Science 120, 4107–4116 Published by The Company of Biologists 2007
doi:10.1242/jcs.012237

Summary

Mutations within connexin50 (Cx50) have been linked to various cataract phenotypes. To determine the mechanism behind cataract formation we used the paired *Xenopus* oocyte system in conjunction with transfected HeLa cells and genetically engineered mouse models to examine the functional characteristics of gap junctions in which a cataract-causing mutant of Cx50 (hereafter referred to as Cx50-S50P) is expressed. Channels comprising Cx50-S50P subunits alone failed to induce electrical coupling. However, the mixed expression of Cx50-S50P and wild-type subunits of either Cx50 or Cx46 – to create heteromeric gap junctions – resulted in functional intercellular channels with altered voltage-gating properties compared with homotypic wild-type channels. Additionally, immunofluorescence microscopy showed that channels of Cx50-S50P subunits alone failed to localize to the plasma

membrane – unlike channels composed of Cx46 subunits, which concentrated at cell-cell appositions. Cx50-S50P colocalized with wild-type Cx46 in both transfected HeLa cells in vitro and mouse lens sections in vivo. Taken together, these data define the electrophysiological properties and intracellular targeting of gap junctions formed by the heteromeric combination of Cx50 or Cx46 and Cx50-S50P mutant proteins. Additionally, mixed channels displayed significantly altered gating properties, a phenomenon that may contribute to the cataract that is associated with this mutation.

Supplementary material available online at
<http://jcs.biologists.org/cgi/content/full/120/23/4107/DC1>

Key words: Cataract, Mutation, Connexin, Gating, Lens

Introduction

Gap junctions provide a vital pathway for the intercellular transport of the ions and small molecules essential for correct growth and development of multicellular organisms (Bruzzone et al., 1996; Evans and Martin, 2002; Harris, 2001). The structural and, thus, physiological diversity of gap junctions are dependent on the specific connexins expressed in the channel. Currently, the connexin gene family contains over 20 members that are expressed in an overlapping, tissue-dependent pattern (Gerido and White, 2004; Willecke et al., 2002). Each connexin contains a cytosolic N- and C-terminus, as well as four transmembrane domains, linked by a single cytoplasmic loop and the two extracellular loops E1 and E2 (Makowski et al., 1977; Milks et al., 1988). Six connexin proteins oligomerize to form a connexon or hemichannel in the plasma membrane. Hemichannels can be of uniform (homomeric) or varying (heteromeric) connexin composition. Neighboring cells may contribute heteromeric or homomeric connexons to form complete intercellular channels known as homotypic (the combination of two identical uniform connexons), heteromeric (the association of two hemichannels varying in connexin expression), and heterotypic channels (the alignment of two connexons each containing a single unique connexin). Recent studies have shown that altering the connexin composition of gap junctions changes both the permeability and electrophysiological properties of these channels in vitro (Bevans et al., 1998; Cao et al., 1998; Donaldson et al., 1995;

Goldberg et al., 1999; Niessen et al., 2000; Valiunas et al., 2002; Veenstra, 1996; White, 2003; White and Bruzzone, 1996).

The vertebrate lens is a functional syncytium connected by gap junctions. In the mammalian lens three connexin family members exhibit distinct but overlapping expression patterns, facilitating the intercellular communication essential to proper organ function. Cx43 is expressed primarily in the epithelium but absent from lens fibers, whereas Cx46 exhibits the opposite expression pattern – as it is found exclusively in lens fiber cells (Gong et al., 1997; Paul et al., 1991). Conversely, Cx50 is present in both, the epithelium and differentiated fibers (Rong et al., 2002; White et al., 1992). This overlapping, yet distinct, pattern of connexin expression contributes to a variation in junctional communication based on the connexin composition in specific cell types (Donaldson et al., 2001; Donaldson et al., 1995; Mathias et al., 1997).

Mutations within the Cx46 and Cx50 gene loci have been linked to various cataract phenotypes in humans and mice (Chang et al., 2002; Graw et al., 2001; Mackay et al., 1999; Runge et al., 1992; Shiels et al., 1998; Steele et al., 1998; Xia et al., 2006b; Xia et al., 2006a; Xu and Ebihara, 1999). In the coding region of Cx50, one such missense mutation caused the substitution of proline for serine at amino acid 50 (S50P) of the protein (Xia et al., 2006b). Mice expressing this mutated protein (hereafter referred to as Cx50-S50P) exhibit a dominant cataract phenotype signified by altered fiber cell formation,

dense cataract and posterior capsule rupture (Xia et al., 2006b). Here, we hypothesize that the mutant Cx50-S50P subunits interact with wild-type Cx46 and Cx50 subunits to modulate cataract formation through alterations in the electrophysiological gating properties of heteromeric gap junctions formed between two lens fiber cells. To test this hypothesis we used the dual whole-cell voltage-clamp technique in conjunction with the paired *Xenopus* oocyte system, and transfected HeLa cells to identify alterations in protein localization and the voltage-gating characteristics of gap junctions comprising wild-type and/or Cx50-S50P mutant subunits.

Results

Connexin expression in *Xenopus* oocytes

The production of lens fiber connexins in *Xenopus* oocytes was examined via immunoblot analysis. Oocytes injected with water, wild-type Cx50, Cx46 or Cx50-S50P alone and cells expressing both mutant and wild-type connexins were analyzed using a polyclonal antibody specific for the central cytoplasmic loop of mouse Cx50 (White et al., 1992) or a polyclonal Cx46 antibody raised against the extreme C-terminus (Paul et al., 1991). Immunoblotting revealed a ~60 kDa band corresponding to Cx50 in oocyte samples injected with wild-type or mutant cRNA transcripts (Fig. 1A). An antibody specific for Cx46 detected two bands of ~46 kDa in samples injected with either Cx46 cRNA alone or co-injected with Cx46 and Cx50-S50P (Fig. 1B). Expression levels were quantified using band densitometry on replicate immunoblots ($n=3$). A plot of the mean band-intensity values (normalized to wild-type mean value) (Fig. 1C) showed no significant reduction of Cx50 expression in oocytes injected with wild-type Cx50 or with Cx50-S50P alone, or co-injected samples expressing both wild-type and mutant Cx50 proteins ($P>0.05$, Student's *t*-test). Similarly, samples tested for Cx46 expression show equivalent levels of Cx46 production (Fig. 1D) in samples injected with Cx46 alone or in conjunction with Cx50-S50P, as band densitometry showed no significant change in mean band intensity ($P>0.05$, Student's *t*-test). Thus, both wild-type and mutant transcripts were synthesized equally and any alteration in channel function cannot be attributed to differences in protein expression.

Cx50-S50P fails to form functional channels in *Xenopus* oocytes

To test the hypothesis that the S50P mutation alters intercellular communication in the lens we measured gap-junctional conductance G_j in oocyte pairs injected with various combinations of lens fiber connexin cRNAs (Fig. 1E). Control oocyte pairs injected with anti-sense oligonucleotide and water showed negligible junctional conductance. By contrast, homotypic wild-type Cx50 or Cx46 channels displayed mean conductance values of ~26 μ S or ~20 μ S, respectively, a significant increase in G_j and several 100-fold greater than that of the background ($P<0.05$, Student's *t*-test). Interestingly, cells injected with both wild-type and mutant Cx50 cRNA transcripts paired to form heteromeric channels, exhibit a mean G_j of ~20 μ S, which was not significantly different compared with homotypic Cx50 channels ($P>0.05$, Student's *t*-test). Similarly, oocytes paired to form heteromeric gap junctions comprising Cx46 and Cx50-S50P subunits displayed a mean

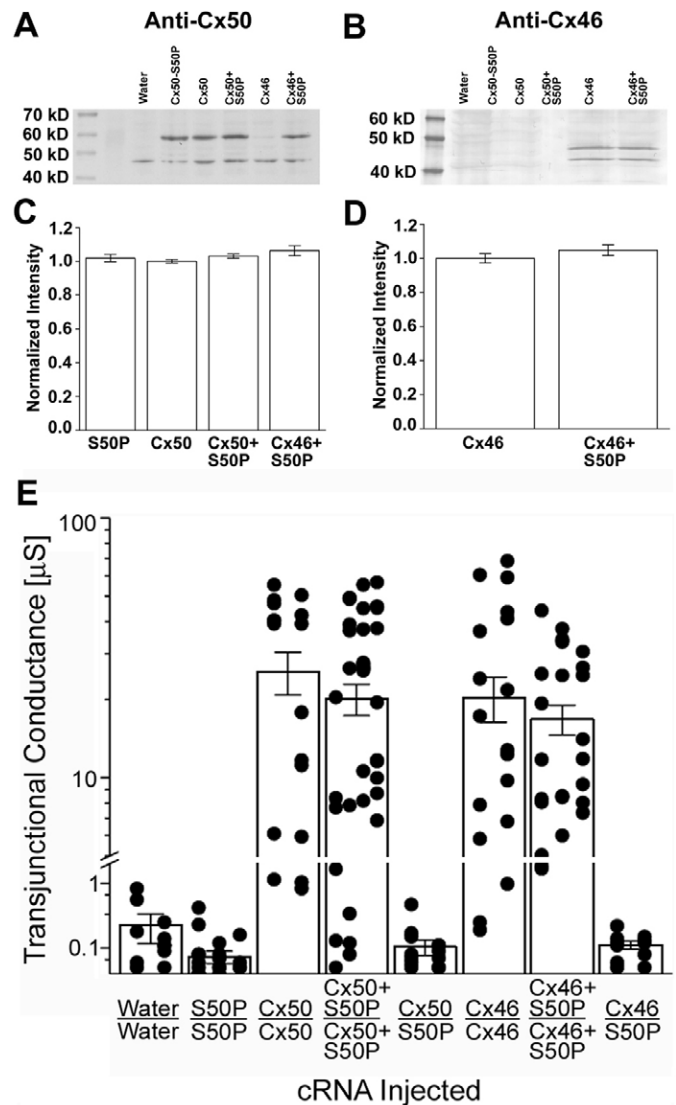


Fig. 1. Cx50-S50P fails to form functional intercellular channels. (A,B) Immunoblot analysis of oocytes showed equivalent levels of wild-type and mutant connexin expression for all conditions tested. (C,D) Band densitometry quantitatively confirmed that mean protein expression was not significantly changed ($P>0.05$, Student's *t*-test). (E) Junctional conductance measurements recorded from *Xenopus* oocyte pairs injected with wild-type Cx50, Cx46 or S50P transcripts alone or in combination. Cell pairs expressing wild-type Cx50 or Cx46 subunits alone form functional gap junctions with mean conductance values of ~26 μ S or ~20 μ S, respectively. Oocytes co-injected with both wild-type and mutant Cx50 transcripts formed channels that displayed a ~20% decrease in G_j when compared with homotypic Cx50 gap junctions, a level of coupling significantly higher than that of the background ($P<0.05$, Student's *t*-test) but not significantly different from homotypic Cx50 channels ($P>0.05$, Student's *t*-test). Similarly, the co-expression of Cx46 and Cx50-S50P subunits did not significantly alter junctional conductance ($P>0.05$, Student's *t*-test) as these channels exhibited a mean G_j of 17 μ S. Heterotypic channels failed to form functional channels with levels of conductance significantly higher than that of the water injected negative controls ($P>0.05$, Student's *t*-test). Cx50-S50P subunits alone failed to produce functional intercellular channels. Data points represent individual conductance measurements. Columns indicate the mean \pm s.e.m.

conductance of 17 μS , a decrease in G_j not significantly different compared with the homotypic Cx46 channel ($P>0.05$, Student's *t*-test). Homotypic channels that comprise mutant Cx50-S50P subunits produced a level of conductance significantly lower than that of homotypic wild-type Cx50, indicating that Cx50-S50P proteins alone fail to form functional intercellular channels ($P<0.05$, Student's *t*-test). Additionally, the heterotypic pairing of oocytes expressing Cx50 or Cx46 with those containing Cx50-S50P alone failed to significantly couple cells, because levels of junctional conductance were similar to that of the background measured in water-injected pairs. Co-injection of Cx50-S50P with wild-type Cx50 or Cx46 facilitated the formation of functional intercellular channels that displayed slight reductions in mean conductance compared with homotypic wild type. These results show that mutant Cx50 subunits fail to form homotypic or heterotypic gap junctions on their own, and do not significantly inhibit conductance when co-expressed with wild-type lens fiber connexins.

Voltage-gating behavior of wild-type and heteromeric channels

To characterize the electrophysiological properties of homotypic wild-type channels or heteromeric channels expressing both wild-type and mutant connexins, voltage-gating was examined by subjecting oocyte pairs to a series of hyperpolarizing and depolarizing transjunctional voltages (V_j). Fig. 2 shows a comparison of representative traces of junctional currents (I_j) for oocyte pairs expressing homotypic Cx50 (Fig. 2A), and mixed-gap-junction-expressing wild-type and mutant Cx50 proteins (Fig. 2B). I_j decreased symmetrically with time in a voltage-dependent manner for both channel types, and showed a more rapid current decline at greater V_j applications. To analyze channel closure kinetics, the initial 250 mseconds of the decay of current was plotted against time and fit to a mono-exponential function to determine the time constant τ . Representative decays of current were recorded during an application of a +80 mV voltage step for homotypic wild-type (Fig. 2C) and mixed channels that express both wild-type Cx50 and mutant subunits (Fig. 2D). Mixed channels closed 15% faster than wild-type channels, with mean channel closure times of 61 vs 52 mseconds, respectively ($P<0.05$). At a larger transjunctional potential of 120 mV, both channel configurations closed faster than at 80 mV, exhibiting mean τ values of 34 and 25 mseconds for homotypic wild-type (Fig. 2E) and co-injected (Fig. 2F) channels, respectively ($P<0.05$, Student's *t*-test). These slight alterations in channel closure kinetics might indicate an interaction between Cx50-S50P and wild-type Cx50 subunits when the two proteins are co-expressed in cells.

The comparison of homotypic channels comprising Cx46 (Fig. 3A) and heteromeric channels comprising Cx46 and Cx50-S50P subunits (Fig. 3B) revealed that heteromeric channels appear to be more sensitive at larger voltage applications (± 80 -120 mV) than their homotypic counterparts. Similarly, mixed channels expressing wild-type Cx46 and Cx50 (Fig. 3C) showed that larger voltage potentials result in a more rapid decline towards steady-state when compared with heteromeric gap junctions containing wild-type Cx46 and Cx50-S50P subunits. Comparison of the three representative I_j decays, Cx46 alone (Fig. 3D), gap junctions expressing both

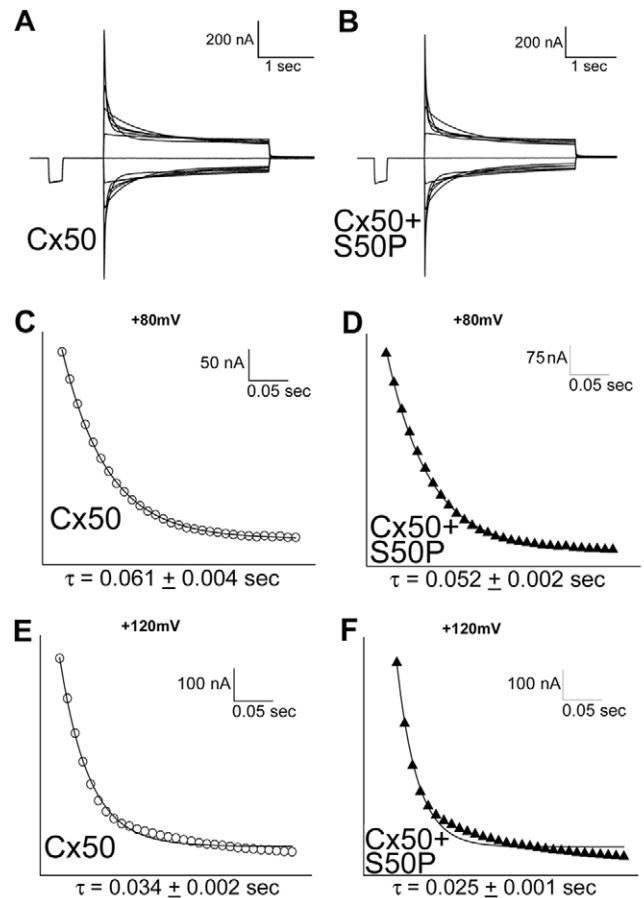
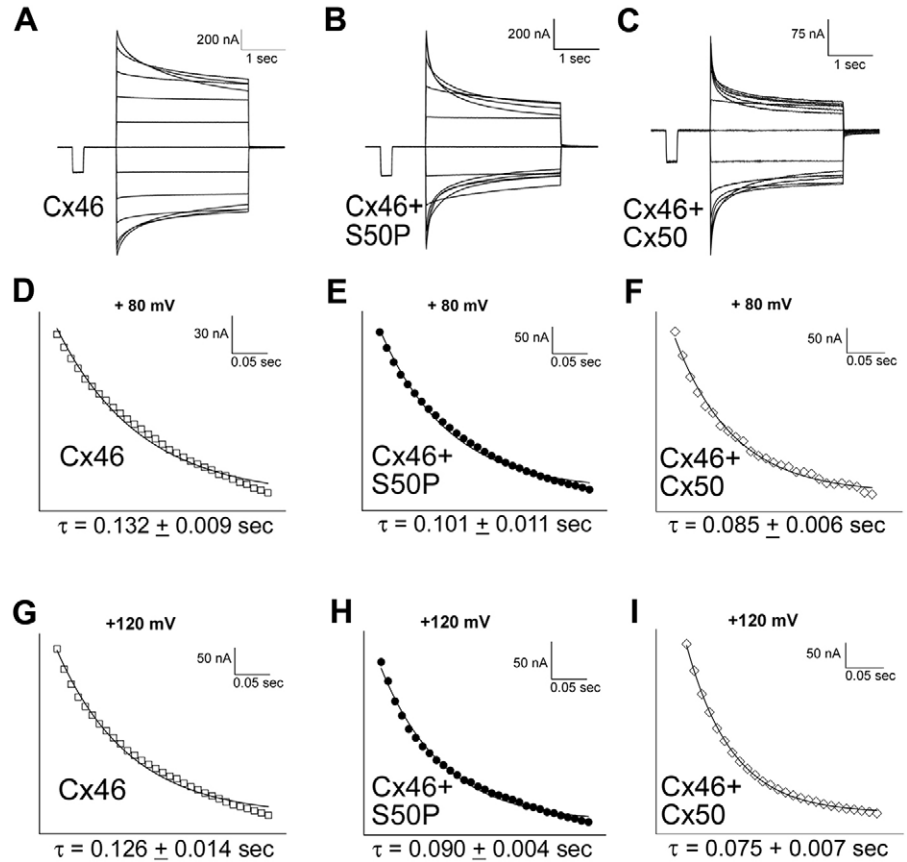


Fig. 2. Voltage-gating properties of homotypic wild-type Cx50 channels and channels co-expressing Cx50-S50P and wild-type Cx50 subunits. (A,B) Junctional current was measured and plotted as a function of time, showing that channels co-expressing (B) both wild-type and mutant Cx50 proteins did not visibly alter current decay when compared with (A) homotypic Cx50 channels. (C) Analysis of channel closure kinetics. Representative current traces plotting the initial 250 mseconds of I_j recordings were fit to a monoexponential decay to determine the mean time constant τ . The co-expression of (C) wild-type and mutant Cx50 transcripts produce a mean τ value of 52 ms ($n=5$) a value significantly different ($P<0.05$, Student's *t*-test) from the 61 msecond mean channel closure time ($n=4$) exhibited by the homotypic wild-type channel during an 80 mV potential. I_j measurements recorded during a 120 mV voltage application show a significant decrease in the mean τ values from 34 mseconds for the (E) homotypic wild-type channel ($n=4$) to 25 ms shown by the (F) co-injected gap junctions ($n=5$, $P<0.05$, Student's *t*-test).

Cx46 and Cx50-S50P proteins (Fig. 3E) and channels comprising wild-type Cx46 and Cx50 (Fig. 3F), using one-way analysis of variance (ANOVA) during an 80 mV voltage application reveal that there were statistically significant differences ($P<0.05$, ANOVA) in the mean channel closure times for all three channel types analyzed. Similarly, when a 120 mV potential was applied to oocyte pairs connected by homotypic Cx46 gap junctions a mean channel closure time of 126 mseconds was recorded (Fig. 3G). Comparison of this τ value with channels comprising wild-type Cx46 and Cx50-S50P (90 mseconds, Fig. 3H), and channels comprising wild-types Cx50 and Cx46 (75 mseconds, Fig. 3I) showed that there

Fig. 3. Voltage-gating properties of homotypic and heteromeric Cx46 channels. (A-C) I_j values recorded from oocyte pairs were plotted as a function of time to reveal that channels expressing (A) wild-type Cx46 alone and mixed channels containing (B) both Cx46 and Cx50-S50P proteins as well as channels expressing (C) wild-type Cx46 and Cx50 subunits displayed altered voltage-gating sensitivity as co-injected pairs appear more responsive at larger voltage applications. Analysis of channel closure kinetics. The initial 250 mseconds of junctional current was fit to a monoexponential decay model to determine the mean time constant τ . (E,D) Representative I_j decays show that during an +80 mV potential channels containing (E) both Cx46 and Cx50-S50P subunits closed in 101 mseconds a value significantly faster than the 132 mseconds mean τ value exhibited by the (D) homotypic Cx46 channel ($P>0.05$, ANOVA). (F) Interestingly, channels co-expressing both wild-type Cx46 and Cx50 closed in 85 mseconds, a rate approximately 16% or 36% faster than the mixed channels containing Cx46 and S50P or homotypic Cx46 gap junctions, respectively. (G,H) Similarly, when a 120 mV V_j was applied, homotypic Cx46 channels closed in 126 mseconds (G), a mean channel closure time significantly slower than the 90 mseconds exhibited by the mixed channels containing wild-type Cx46 and S50P proteins (H) ($P>0.05$, ANOVA). Heteromeric channels containing both wild-type Cx46 and Cx50 (I), displayed a mean τ value of 75 mseconds, a closure speed that is significantly faster than either the homotypic Cx46 or heteromeric Cx46 and S50P channel ($P>0.05$, ANOVA). All means are the sum of four independent experiments.



were statistically significant differences between the three mean τ values ($P<0.05$, ANOVA). Thus, the behavior of mixed channels containing wild-type Cx46 and Cx50-S50P was functionally distinct from either homotypic Cx46 channels or heteromeric gap junctions expressing wild-type Cx46 and Cx50 subunits. These data support the hypothesis that Cx50-S50P interacts with wild-type Cx46 to form functional gap junctions with unique voltage gating properties.

The steady-state voltage gating behavior of these channels was examined by plotting V_j against G_j (normalized to the values obtained at ± 20 mV) and fitting the data to the Boltzmann equation (Fig. 4, Table 1). Analysis of the equilibrium gating properties showed no drastic changes in the steady-state properties of homotypic Cx50 channels and mixed gap junctions co-expressing wild-type and mutant Cx50 (Fig. 4A). Conversely, mixed channels containing both Cx46 and Cx50-S50P subunits (Fig. 4B, ●) displayed a visible shift towards lower transjunctional voltages in the Boltzmann plot when compared with wild-type Cx46 channels (Fig. 4B, □), indicating that heteromeric channels were more voltage sensitive than the homotypic wild-type Cx46 junctions at all tested voltages. Heteromeric channels that comprised wild-type Cx46 and Cx50 (Fig. 4B, ◇) were similar to those containing Cx46 and Cx50-S50P at negative transjunctional potentials, but showed a statistically significant alteration in voltage sensitivity at larger positive potentials (Fig. 4B, *).

One-way analysis of variance (ANOVA) revealed that there were statistically significant differences between all three data sets at all positive potentials ≥ 60 mV ($P<0.05$).

Taken together, these results provided evidence for the heteromeric interaction between wild-type lens fiber connexins and mutant Cx50-S50P subunits in vitro. Interestingly, the co-expression of wild-type Cx46 and Cx50-S50P presented strong evidence for the functional interaction between these two proteins via, the formation of functional intercellular channels with decreased junctional conductance, visibly altered junctional current decay and significantly altered channel closure kinetics. By contrast, the co-expression of wild-type and mutant Cx50 produced smaller shifts in the electrophysiological properties, although these achieved statistical significance and fully support the interaction of wild-type Cx50 and Cx50-S50P subunits in vitro.

Voltage-gating behavior of heterotypic channels

To determine whether the slight shift in mean channel closure time and the 20% reduction in conductance could be attributed to interaction of the Cx50-S50P mutant with wild-type Cx50, we analyzed the voltage gating characteristics of heterotypic channels where homomeric Cx46 connexons were paired with either Cx50 homomeric hemichannels or heteromeric connexons containing both wild-type and mutant Cx50 subunits. Junctional conductance measurements recorded from

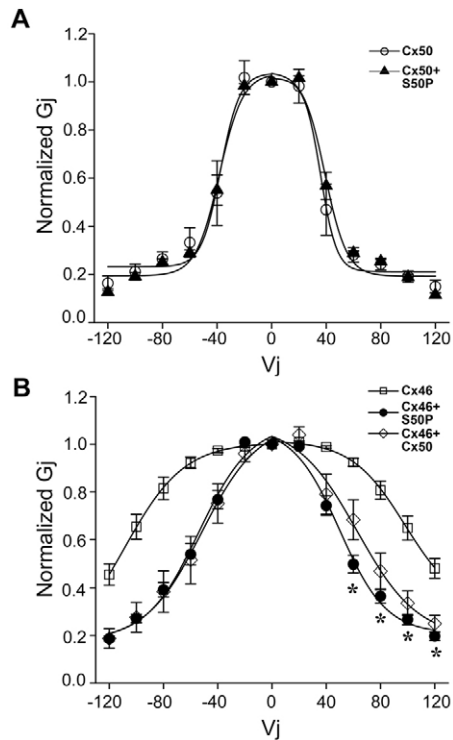


Fig. 4. Comparison of steady-state conductance properties. Equilibrium gating properties were analyzed by plotting normalized junctional conductance against transjunctional voltage and fit to the Boltzmann equation. (A) comparison of homotypic wild-type Cx50 channels ($n=4$) and mixed gap junctions containing both wild-type and mutant Cx50 subunits ($n=6$) showed similar voltage sensitivity, as indicated by the overlapping pattern of the two Boltzmann plots. The steady-state reduction in conductance was greater for mixed channels expressing both Cx46 and S50P subunits ($n=8$) when compared with that of the homotypic Cx46 channel ($n=4$), indicating an increase in voltage gating sensitivity for heteromeric channels. (B) Equilibrium gating properties displayed modest changes at positive potentials when mixed channels containing both wild-type Cx46 and Cx50 ($n=6$) were compared with heteromeric channels expressing wild-type Cx46 and S50P. Results are shown as the mean \pm s.e.m.

oocytes paired to form heterotypic channels (Fig. 5A) showed that heterotypic gap junctions containing only wild-type Cx46 and Cx50 display a mean G_j value of $\sim 22 \mu\text{S}$ a significant increase in coupling when compared to the $10.5 \mu\text{S}$ exhibited by heterotypic channels containing wild-type and mutant Cx50 subunits ($P < 0.05$, Student's t -test). Both channel types displayed a level of conductance significantly higher than that of the water injected negative controls ($P < 0.05$, Student's t -test). Representative current traces for heterotypic oocyte pairs derived from cells expressing only Cx46 and paired with Cx50 alone (Fig. 5B), or oocytes co-expressing both wild-type and mutant Cx50 transcripts (Fig. 5C) exhibit no obvious changes in junctional current decay for all voltage applications assayed. To analyze the gating properties of heterotypic gap junctions, equilibrium gating properties of these channels were analyzed by applying the Boltzmann equation (Fig. 5D). Heterotypic channels expressing both wild-type and mutant Cx50 proteins showed a slight, but statistically significant increase in voltage dependence compared with heterotypic

Table 1. Boltzmann parameters for wild-type and mixed channels

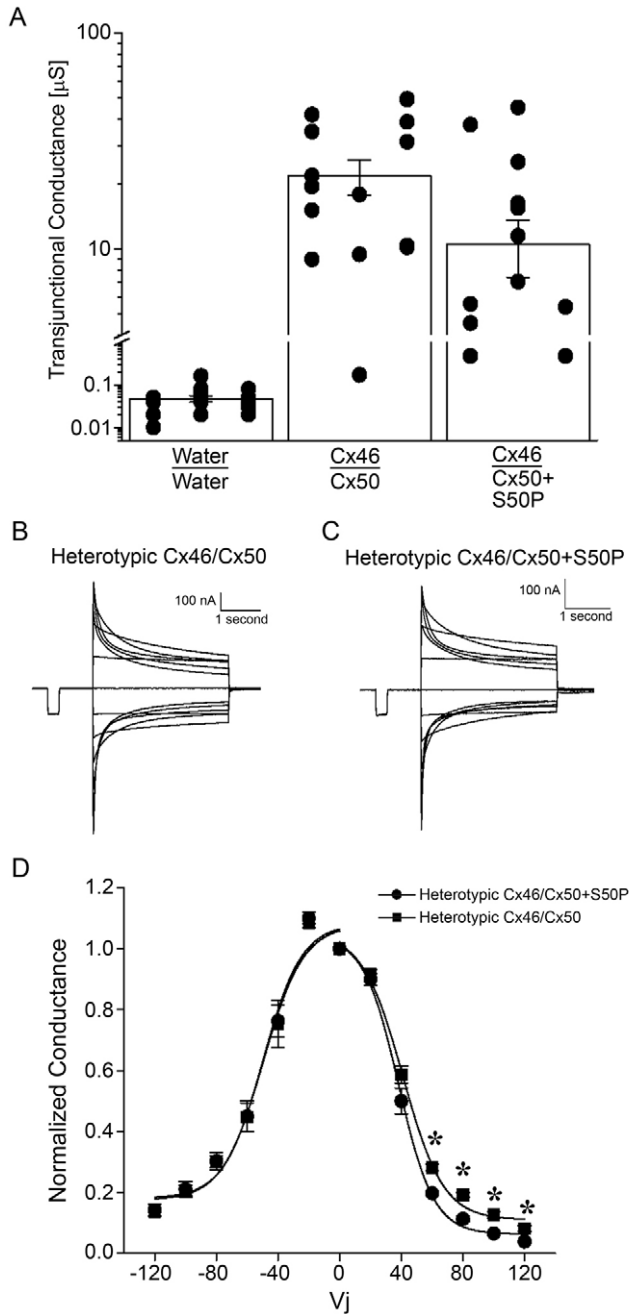
Connexon	V_j	V_0	$G_{j\text{min}}$	A
Homotypic				
Cx50	+	36	0.21	0.21
Cx50	-	-37	0.23	0.18
Cx46	+	98	0.31	0.07
Cx46	-	-108	0.13	0.05
Heteromeric				
Cx50 + Cx50-S50P	+	39	0.19	0.15
Cx50 + Cx50-S50P	-	-38	0.19	0.14
Cx46 + Cx50-S50P	+	50	0.21	0.07
Cx46 + Cx50-S50P	-	-54	0.18	0.07
Cx46 + Cx50	+	63	0.19	0.06
Cx46 + Cx50	-	-52	0.17	0.06
Heterotypic				
Cx46	-	-50	0.18	0.07
Cx50	+	41	0.11	0.07
Cx50 + Cx50-S50P	+	38	0.06	0.09

$G_{j\text{min}}$, minimum conductance value; V_0 , voltage measured midway through the G_j decline; A, cooperativity constant, reflecting the number of charges moving through the transjunctional field. $+V_j$ and $-V_j$ indicate transjunctional membrane potential polarity.

channels expressing wild-type Cx46 and Cx50 proteins alone, as indicated by the downward shift in the Boltzmann curve for positive values of V_j ($*P < 0.05$, Student's t -test, Table 1). Taken together, these data indicate that the reduction in G_j that is seen in mixed channels comprising wild-type and mutant Cx50 proteins, as well as the slight alteration in voltage sensitivity was owing to the heteromeric interaction of CX50-S50P with wild-type Cx50.

Cx50-S50P requires Cx46 to form voltage-sensitive hemichannels

Several studies have suggested that abnormal hemichannel activity plays a role in the development of connexin-related diseases (Gerido et al., 2007; Jiang and Gu, 2005), and Cx46 and Cx50 have both been shown to form hemichannels in vitro (Beahm and Hall, 2002; Ebihara and Steiner, 1993). To test whether Cx50-S50P forms functional hemichannels that might have contributed to the mutant lens phenotypes seen in vivo, whole-cell currents (I_m) were recorded from single oocytes expressing wild-type Cx46 or Cx50-S50P proteins alone or in combination (supplementary material Fig. S1). Oocytes expressing wild-type Cx46 alone revealed slowly activated outward currents that increased as voltage applications became larger and more positive. Conversely, CX50-S50P-injected oocytes exhibited negligible current flow at all voltage potentials analyzed. Mixed expression of wild-type Cx46 and Cx50, or wild-type Cx46 and CX50-S50P similarly displayed the presence of intermediate outward currents for both tested conditions. When steady-state currents were plotted against membrane voltage, negligible membrane currents were displayed by cells expressing only Cx50-S50P, whereas cells injected with wild-type Cx46 transcripts exhibited large currents that increased with V_m . Reduced whole-cell currents were observed for cells expressing both wild-type lens fiber connexins as well as cells containing wild-type Cx46 and CX50-S50P proteins. These data suggest that CX50-S50P fails to form hemichannels alone, but can form heteromeric hemichannels with wild-type Cx46.



Aberrant localization of Cx50-S50P in transfected cells and in the lens

It has been previously reported that mutant Cx50 proteins exhibited altered abilities to localize to the cell membrane as well as a reduced capacity to form gap-junctional plaques (Chang et al., 2002; Xia et al., 2006a). To determine whether the reductions in junctional conductance shown by channels of mixed connexin expression was the result of a failure to efficiently localize connexins to the plasma membrane, wild-type Cx46, and/or Cx50-S50P (subcloned into the pIRES2-EGFP and pCS2+ vectors, respectively) were expressed in transiently transfected HeLa cells.

Immunofluorescent images revealed sufficient connexin expression for both wild-type Cx46 (Fig. 6B and 6D) and

Fig. 5. Gating analysis of heterotypic wild-type and co-injected channels. G_j measurements recorded from oocyte paired to form heterotypic wild-type or co-injected gap junctions. (A) Cell pairs expressing wild-type Cx46 and Cx50 subunits form functional gap junctions with mean conductance values of $\sim 22 \mu\text{S}$, a level of coupling significantly higher than that of the water-injected negative control ($P < 0.05$, Student's t -test). Co-injected heterotypic channels that expressed both wild-type and mutant Cx50 transcripts formed channels that displayed a $\sim 50\%$ decrease in G_j when compared with wild-type heterotypic gap junctions, a level of coupling significantly higher than that of the background ($P < 0.05$, Student's t -test). Data points represent individual conductance measurements. Columns indicate the mean \pm s.e.m. (B,C) Junctional currents recorded from oocyte pairs were plotted as a function of time to compare heterotypic gap junctions expressing (B) wild-type Cx46 and Cx50 subunits and (C) heterotypic channels containing wild-type Cx46 and wild-type Cx50 and S50P mutant proteins. Representative I_j decays revealed that co-injected pairs appear more responsive at greater depolarizing voltage applications as well as more asymmetric than heterotypic channels comprising wild-type lens fiber connexins. Comparison of steady-state conductance properties. Equilibrium gating properties were analyzed by plotting normalized junctional conductance against transjunctional voltage and fit to the Boltzmann equation. (D) The steady-state reduction in conductance was greater for channels expressing both wild-type Cx50 and Cx50-S50P subunits ($n=6$) when compared with that of the heterotypic wild-type channel ($n=5$), indicating an increase in voltage-gating sensitivity for heterotypic channels containing the mutant protein.

Cx50-S50P (Fig. 6A and 6C) proteins. Cx50-S50P alone was unable to localize to sites of cell-cell apposition (Fig. 6, arrows), instead accumulating in subcellular compartments surrounding the nucleus (Fig. 6A). Conversely, Cx46 subunits were properly targeted to plasma membrane regions of cell-to-cell interaction in 75% of the cell pairs analyzed (Table 2), a phenomenon consistent with the formation of gap junctions (Fig. 6B, arrowhead). Interestingly, co-transfection of HeLa cells with both wild-type Cx46 and Cx50-S50P cDNA facilitated the colocalization of these proteins in 74% of the cell pairs examined (Fig. 6C and 6D).

Immunostaining of frozen lens sections further confirmed the notion that Cx50-S50P mutant proteins were stabilized in gap junction plaques by Cx46 in vivo. Fluorescent images showed that Cx50-S50P mutant proteins were only detected in the most superficial differentiating fiber cells of Cx50^(S50P/S50P)-Cx46^(-/-) lenses both lacking endogenous wild-type Cx50 and Cx46 alleles (Fig. 6F). Conversely, substantial staining was extended deeper into differentiating fibers of Cx50^(S50P/S50P)-Cx46^(+/+) lenses that expressed endogenous wild-type Cx46 (Fig. 6E). Thus, both in vivo and in vitro findings support the hypothesis that the mutant Cx50-S50P protein has the ability to associate with wild-type Cx46 subunits, a phenomenon that might play a role in cataract formation.

Table 2. Quantitative analysis of gap junctional plaque formation in transiently transfected HeLa cells

Connexin expressed	Junctional plaques present	No junctional plaques	Number of cell pairs analyzed
Cx50-S50P	0	18	18
Wild-type Cx46	12	4	16
Cx46 + Cx50-S50P	14	5	19

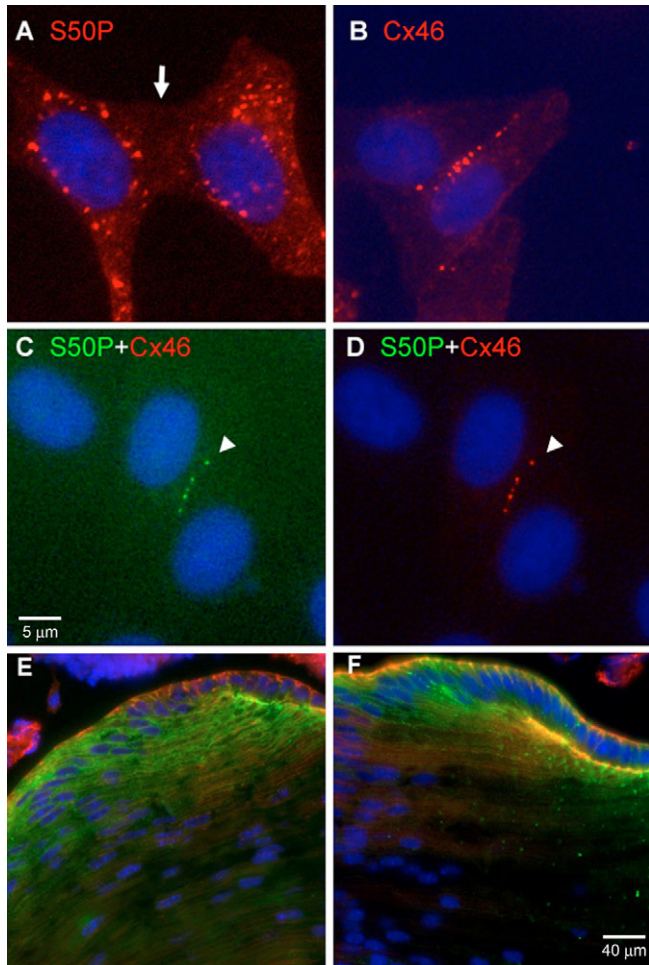


Fig. 6. Immunofluorescent imaging of Cx50-S50P *in vitro* and *in vivo*. (A,B) Transiently transfected HeLa cells expressing (A) Cx50-S50P or (B) wild-type Cx46 proteins were immunostained and examined by fluorescence microscopy. Merged images taken at $\times 100$ (A) and $\times 60$ (B,C,D) exhibit Cy2 (green) and/or Cy3 (red) staining of connexins and DAPI staining of cell nuclei (blue). The images showed that Cx50-S50P alone fails to correctly localize to the cell membrane, instead showing the accumulation of connexin subunits in subcellular compartments surrounding the nucleus (A). Wild-type Cx46 was efficiently translated and localized to the membrane specifically at areas of cell to cell apposition (B, arrow). (C,D) HeLa cells cotransfected with both Cx50-S50P (C) and wild-type Cx46 (D) showed that in the presence of Cx46, S50P subunits were colocalized to the membrane and form junctional plaques with at areas of cell-cell contact. (E,F) Fluorescence images of Cx50-S50P immunostaining in the bow region of homozygous mutant lenses (E) with Cx46 (Cx50^(S50P/S50P)-Cx46^(+/+)) and (F) without endogenous Cx46 (Cx50^(S50P/S50P)-Cx46^(-/-)). These lenses taken from mice on postnatal day 7 showed more punctate Cx50 staining (green) which extended deeper into the lens differentiating fibers in the presence of wild-type Cx46 proteins. Frozen Lens sections were co-stained with Rhodamine-phalloidin (red) and DAPI (blue). Bars, 5 μm (A-D), 40 μm (E-F).

Discussion

In this study, we have used a dual whole-cell voltage clamp method to characterize the electrophysiological properties of gap-junctional channels between paired *Xenopus* oocytes

injected with different combinations of wild-type and mutant connexins. Dual whole-cell voltage clamp has been extensively used to analyze and obtain unique 'electrical fingerprints' as a means of identifying functional differences between intercellular channels composed from diverse connexin subunits (Bruzzone et al., 1996; Harris, 2001). Whereas the transjunctional potentials created using this assay may not correlate with the endogenous resting potentials present in the mammalian lens, the distinct functional characteristics revealed by these techniques have enabled the detection of changes in intrinsic channel properties that could only result from the interaction of the Cx50-S50P mutant with wild-type Cx46 and Cx50. These functional interactions have been used to generate a model to explain the physiological pathologies that occur *in vivo*.

The data presented herein provide *in vitro* and *in vivo* evidence for the interaction between wild-type Cx50, wild-type Cx46 and mutant Cx50-S50P subunits. Furthermore, this study provides support for the hypothesis that a unique interaction between mutant and wild-type lens connexins modulates the aberrant lens phenotypes displayed by Cx50-S50P mutant mice (Xia et al., 2006b). Our findings showed that, although Cx50-S50P subunits alone failed to form functional intercellular channels or voltage activated hemichannels in *Xenopus* oocytes, or target to gap junctions in transfected HeLa cells, upon the mixed expression of wild-type lens fiber connexins and mutant Cx50-S50P subunits they were able to form functional gap junctions, and displayed levels of electrical coupling comparable to those recorded from homotypic wild-type channels. Additionally, heteromeric channels comprising either wild-type Cx46 or Cx50 and S50P proteins exhibited distinct voltage gating properties, and increased the ability of the mutant to localize in junctional plaques. Together, these data imply that unique interactions between connexins in the lens play a crucial role in correct organ function and development.

Recent studies have revealed that connexin diversity plays an integral role in the correct development and function of the mammalian lens, contributing to changes in channel gating and permeation (Gao et al., 2004; Le and Musil, 2001; Martinez-Wittinghan et al., 2003; Rong et al., 2002; White, 2003). In the past, different Cx50 variants have been described in the development of several distinct types of dominant cataract in mice (Chang et al., 2002; Graw et al., 2001; Steele et al., 1998; Xia et al., 2006a). For instance, recently published data revealed that the combination of mutants Cx50-G22R (Xia et al., 2006a) or Cx50-S50P (Xia et al., 2006b) and wild-type lens fiber connexins led to unique aberrations in lens development and function, and the presence of these mutant subunits in gap junction channels led to alterations in channel gating properties and cell-cell communication *in vitro*. Similarly, mice heterozygous for the S50P mutation showed a unique deficiency in primary fiber cell elongation indicating that an interaction between the wild-type and mutant Cx50 subunits governs primary fiber cell development, whereas homozygous mutant mice exhibited lenses with a unique deficiency in secondary fiber cell development, a finding that suggest involvement of Cx50 in a separate mechanism (Fig. 7) that modulates secondary fiber cell development (Gong et al., 2007; Xia et al., 2006b). Since the S50P mutant alone has been shown to be nonfunctional and failed to properly localize to the








Embryonic lens	Embryonic phenotype, proposed mechanism	Postnatal lens	Adult phenotype, proposed mechanism
	abberant primary fiber cell elongation		small lenses, with malformed secondary fibers and posterior capsule rupture
Cx50^(S50P/+) Cx46^(-/-) Cx50^(S50P/+) Cx46^(+/+)	co-expression of wild-type and mutant Cx50 alters channel function	Cx50^(S50P/-) Cx46^(+/+)	co-expression of S50P and Cx46 form channels with altered function and gating properties, affecting only postnatal development
	normal embryonic development		small lenses with altered primary and secondary fibers
Cx50^(S50P/-) Cx46^(+/+)	mixing of S50P and wild-type Cx46 alters channel function without affecting embryonic development	Cx50^(S50P/+) Cx46^(+/+)	the presence of S50P and wild-type lens connexins leads to altered channel function affecting both embryonic and postnatal development
	normal embryonic development		small lenses with normal secondary fibers and disorganized primary fiber cells
Cx50^(S50P/-) Cx46^(-/-) Cx50^(-/-) Cx46^(-/-)	the expression of S50P alone does not affect embryonic lens development, similar to double knockout lens	Cx50^(S50P/+) Cx46^(-/-)	mixing of wild-type and mutant Cx50 forms channels with altered gating properties that does not affect secondary fiber development
			small lenses with normal peripheral fibers and degenerate primary fiber cells, dense nuclear cataract
		Cx50^(S50P/-) Cx46^(-/-) Cx50^(-/-) Cx46^(-/-)	S50P alone is a loss of function mutation that fails to form functional gap junctions producing a phenotype identical to that of the double knockout lens

Fig. 7. Description of embryonic and adult lens phenotypes produced by mixing Cx50-S50P and wild-type lens fiber connexins. This model describes the embryonic and postnatal phenotypes of various mouse lenses created by breeding heterozygous mutant (Cx50^(S50P/+)-Cx46^(+/+)) and double knockout (Cx50^(-/-)-Cx46^(-/-)) mice. The drawing explains the proposed mechanism behind development of each unique phenotype based on the electrophysiological interactions documented herein.

membrane (Fig. 1E, Fig. 6), we propose that the mutant must dominantly interact with wild-type subunits to impair lens development *in vivo*. Our results support these hypotheses and also provide the mechanistic foundation for the unique cataract phenotypes exhibited by the S50P mutant mice.

Taken together these data clearly demonstrate that Cx50 plays a crucial part in lens fiber cell development. Heterozygous Cx50^(S50P/+)-Cx46^(-/-) mice display a large cystic lumen between the anterior primary fiber cells and the epithelium during embryonic development, whereas postnatal fiber cell development proceeded normally. We propose that this phenomenon is governed by the unique interaction between the wild-type and mutant Cx50 subunits shown here that led to altered intercellular communication mediated by channels of mixed connexin expression. Moreover, we provide support for the hypothesis that Cx50 also plays a separate distinct role in postnatal fiber cell development *in vivo*. Interestingly, heterozygous Cx50^(S50P/-)-Cx46^(+/+) mice exhibit normal embryonic development in the presence of wild-type Cx46. However, these animals revealed disrupted secondary fiber development as well as the presence of a dense nuclear cataract and posterior capsule rupture. These findings taken in conjunction with the data shown here indicate an essential role

for connexin diversity and Cx50-mediated intercellular communication in postnatal lens development.

In summary, these data indicate that mutated connexin subunits can interact with wild-type lens connexins to modulate both prenatal and postnatal lens development by altering channel function and cell-cell communication. Furthermore, varying the expression of wild-type lens connexins *in vivo* and *in vitro* has shown that wild-type Cx50 interacts with mutant Cx50-S50P in a manner that distinctly affects pre-natal development through a slight alteration in channel gating, whereas a separate unique interaction between Cx50-S50P and wild-type Cx46 impairs postnatal lens fiber development through more profound alterations in intercellular communication. The distinctive properties of the heteromeric channels formed by wild-type and mutant lens connexins provide the basic molecular foundation behind a variety of unique cataract phenotypes attributed to various Cx50 mutations (Arora et al., 2006; Graw et al., 2001; Xia et al., 2006a; Xu and Ebihara, 1999). These data indicate that mutated Cx50 proteins act as the molecular mechanism governing altered function of gap junction channels and aberrant intercellular communication in the lens. We believe that a better understanding of these underlying mechanisms

may lead to the identification of molecular approaches to cataract prevention.

Materials and Methods

Molecular cloning

Murine Cx50 was cloned between the *XhoI-XbaI* sites of the pCS2+ expression vector. Mutant Cx50-S50P cDNA was generated from total mRNAs of homozygous mutant lenses by RT-PCR using a pair of primers (sense 5'-CGGGATCCTAGT-GAGCAATGGGCGAC-3' and anti-sense 5'-GGAATTCGTATGGTGGAG-ATCATC-3'). Mutant cDNA was subcloned into pCR-bluntII-TOPO vector (Invitrogen, Carlsbad, CA) and sequenced to confirm the serine for proline amino acid substitution at position 50. Mutant Cx50-S50P cDNA was further subcloned into the pCS2+ and pIRES2-EGFP (Clontech, Palo Alto, CA) expression vectors using the *EcoRI* restriction sites for expression in *Xenopus laevis*, sequencing and immunofluorescent staining. Wild-type mouse Cx46 was inserted into the pCS2+ expression vector using the *XhoI* and *SpeI* restriction sites.

In-vitro transcription, oocyte microinjection and pairing

The aforementioned wild-type Cx50, Cx46 and mutant Cx50-S50P plasmids were linearized at the *NorI* restriction site of pCS2+, and transcribed using the SP6 mMessage mMachine (Ambion). Adult *Xenopus* females were anesthetized, the ovaries were removed and stage V-VI oocytes were collected after the ovarian lobes were de-folliculated in a solution containing 50 mg/ml collagenase B and 50 mg/ml hyaluronidase in modified Barths medium (MB) without Ca^{2+} . Cells were first injected with 10 ng of antisense *Xenopus* Cx38 oligonucleotide to eliminate coupling caused by endogenous intercellular channels, and cultured overnight in MB medium containing 2 mM of CaCl_2 . Oligonucleotide-injected oocytes were then injected with either wild-type or mutant Cx50 cRNA transcripts (5 ng per cell) alone or in combination or H_2O as a negative control. The vitelline membranes were then removed in a hypertonic solution (200 mM aspartic acid, 10 mM HEPES, 1 mM MgCl_2 , 10 mM EGTA, and 20 mM KCl at pH 7.4), and the oocytes were manually paired with the vegetal poles apposed in either normal MB medium or MB with elevated Ca^{2+} (2 mM CaCl_2).

Dual whole-cell voltage clamping

Following an overnight incubation, gap-junctional coupling between oocyte pairs was measured using the dual whole-cell voltage clamp technique (Bruzzone et al., 2003; Spray et al., 1981). Current and voltage electrodes (1.2-mm diameter, omega dot; Glass Company of America, Millville, NJ) were pulled to a resistance of 1-2 M Ω with a horizontal puller (Narishige, Tokyo, Japan) and filled with solution containing 3 M KCl, 10 mM EGTA, and 10 mM HEPES pH 7.4. Voltage clamp experiments were performed using two GeneClamp 500 amplifiers (Axon Instruments, Foster City, CA) controlled by a PC-compatible computer through a Digidata 1320A interface (Axon Instruments). The pCLAMP 8.0 software (Axon Instruments) was used to program stimulus and data collection paradigms.

For measurements of junctional conductance, cell pairs were first clamped at -40 mV to eliminate any transjunctional potentials. Following the -40 mV clamp, a single cell was subjected to alternating pulses of ± 10 -20 mV, whereas the current produced by the change in voltage was recorded in the second cell. The current delivered to the second cell was equal in magnitude to the junctional current. Junctional conductance was calculated by dividing the measured current by the voltage difference, $G_j = I_j / (V_1 - V_2)$.

To determine voltage-gating properties, transjunctional potentials (V_j) of opposite polarity were generated by hyperpolarizing or depolarizing one cell in 20-mV steps (range: ± 120 mV) while clamping the second cell at -40 mV. Currents were measured at the end of the voltage pulse, at which time they approached steady-state (I_{jss}). Macroscopic conductance (G_{jss}) was calculated by dividing I_{jss} by V_j , normalized to the values determined at ± 20 mV, and plotted against V_j . Data describing the relationship of G_{jss} as a function of V_j were analyzed using Origin 6.1 (Microcal Software, Northampton, MA) and fit to a Boltzmann relation of the form: $G_{jss} = (G_{jmax} - G_{jmin}) / (1 + \exp[A(V_j - V_0)]) + G_{jmin}$, where G_{jss} is the steady-state junctional conductance, G_{jmax} (normalized to unity) is the maximum conductance, G_{jmin} is the residual conductance at large values of V_j , and V_0 is the transjunctional voltage at which $G_{jss} = (G_{jmax} - G_{jmin}) / 2$. The constant $A = nq/kT$ represents the voltage sensitivity in terms of gating charge as the equivalent number (n) of electron charges (q) moving through the membrane, k is the Boltzmann constant, and T is the absolute temperature.

Preparation of oocyte samples for western blots

Oocytes were collected in 1 ml of buffer containing 5 mM Tris pH 8.0, 5 mM EDTA and protease inhibitors (White et al., 1992) and lysed using a series of mechanical passages through needles of diminishing caliber (20, 22 and 26 Ga). Extracts were centrifuged at 1000 g at 4°C for 5 minutes. The supernatant was then centrifuged at 100,000 g at 4°C for 30 minutes. Membrane pellets were resuspended in SDS sample buffer (2 μ l per oocyte), samples were separated on 10% SDS gels and transferred to nitrocellulose membranes. Blots were blocked with 5% BSA in 1 \times PBS with 0.02% NaN_3 for 1 hour and probed with a polyclonal Cx50 antibody,

(White et al., 1992) or a polyclonal Cx46 antibody (Paul et al., 1991) followed by incubation with alkaline-phosphatase conjugated anti-rabbit secondary antibody (Jackson laboratories). Band intensities were quantified using Kodak 1D Image Analysis software (Eastman Kodak, Rochester, NY). Values from four independent experiments were normalized to the mean value of band intensity of the wild-type sample.

Electrophysiological recording of hemichannel currents

Macroscopic recordings of hemichannel currents were obtained from single *Xenopus* oocytes using a GeneClamp 500 amplifier controlled by a Digidata 1320 interface (Axon Instruments, Foster City, CA). pClamp 8.0 software (Axon Instruments) was used to program stimulus and data collection paradigms. To obtain hemichannel I-V curves, cells were initially clamped at -40 mV and subjected to 5-second depolarizing voltage steps ranging from -30 to +60 mV in 10-mV increments. Membrane currents were analyzed by recording hemichannel currents from cells injected with appropriate cRNA transcripts, incubated overnight in MB medium supplemented with 2 mM CaCl_2 .

Transient transfection and immunocytochemical staining

HeLa cells were plated on 22-mm square coverslips and grown to 50% confluence then transiently transfected with 2 μ g of connexin DNA subcloned into the pIRES2-EGFP or pCS2+ vector using Lipofectamine 2000 (Gibco BRL, Gaithersburg, MD). After overnight incubation, cells were fixed with 1% paraformaldehyde in PBS, blocked with 5% BSA in PBS with 0.1% Triton X-100 and 0.02% NaN_3 . Cells were stained with either a polyclonal anti-Cx50 or anti-Cx46 antibody followed by incubation with an anti-Cy3 goat anti-rabbit secondary antibody, or an anti-Cy2 conjugated fluorescent mouse anti-rabbit secondary antibody (Jackson ImmunoResearch Laboratories). HeLa cells expressing wild-type Cx46 or Cx50-S50P cDNA alone were transfected with the subsequent cDNA using pIRES2-EGFP vector and stained with an anti-Cy3 goat anti-rabbit secondary antibody. For co-transfected cells Cx50-S50P and Cx46 constructs were inserted into the pCS2+ vector using the *EcoRI* restriction sites. Co-transfected cells were then treated with a polyclonal mouse anti-rabbit Cx50 antibody or a polyclonal goat anti-rabbit Cx46 primary antibody, followed by incubation with a Cy2 mouse anti-rabbit secondary antibody or Cy3 conjugated goat anti-rabbit antibody, to determine co-localization. Cells were viewed and photographed on an Olympus BX51 microscope using an Optronics MagnaFire digital camera. Gap-junctional plaque formation was quantified by immunofluorescent microscopy. Images were photographed at 60 \times and areas of cell-cell contact were examined for the presence of gap-junctional plaques and counted.

Staining of lens sections

A previously described method was used to prepare frozen lens sections for immunohistochemical analysis (Gong et al., 1997). A rabbit polyclonal antibody against the C-terminal region of Cx50 was generously provided by M. J. Wolosin at Mt Sinai School of Medicine. Sections were counterstained with Rhodamine-phalloidin (Molecular Probe) for detecting F-actin and DAPI (Vector Laboratories) for labeling cell nuclei. Fluorescent images were collected under a Zeiss Axiovert 200 fluorescence microscope with an Axiocam camera.

This work was supported by NIH grants EY13849 (X.G.) and EY13163 (T.W.W.).

References

- Arora, A., Minogue, P. J., Liu, X., Reddy, M. A., Ainsworth, J. R., Bhattacharya, S. S., Webster, A. R., Hunt, D. M., Ebihara, L., Moore, A. T. et al. (2006). A novel GJA8 mutation is associated with autosomal dominant lamellar pulverulent cataract: further evidence for gap junction dysfunction in human cataract. *J. Med. Genet.* **43**, e2.
- Beahm, D. L. and Hall, J. E. (2002). Hemichannel and junctional properties of connexin 50. *Biophys. J.* **82**, 2016-2031.
- Bevans, C. G., Kordel, M., Rhee, S. K. and Harris, A. L. (1998). Isoform composition of connexin channels determines selectivity among second messengers and uncharged molecules. *J. Biol. Chem.* **273**, 2808-2816.
- Bruzzone, R., White, T. W. and Paul, D. L. (1996). Connections with connexins: the molecular basis of direct intercellular signaling. *Eur. J. Biochem.* **238**, 1-27.
- Bruzzone, R., Veronesi, V., Gomes, D., Bicego, M., Duval, N., Marlin, S., Petit, C., D'Andrea, P. and White, T. W. (2003). Loss-of-function and residual channel activity of connexin26 mutations associated with non-syndromic deafness. *FEBS Lett.* **533**, 79-88.
- Cao, F., Eckert, R., Elfgang, C., Nitsche, J. M., Snyder, S. A., Hülser, D. F., Willecke, K. and Nicholson, B. J. (1998). A quantitative analysis of connexin-specific permeability differences of gap junctions expressed in HeLa transfectants and *Xenopus* oocytes. *J. Cell Sci.* **111**, 31-43.
- Chang, B., Wang, X., Hawes, N. L., Ojakian, R., Davisson, M. T., Lo, W. K. and Gong, X. (2002). A Gja8 (Cx50) point mutation causes an alteration of alpha 3 connexin (Cx46) in semi-dominant cataracts of Lop10 mice. *Hum. Mol. Genet.* **11**, 507-513.

- Donaldson, P. J., Dong, Y., Roos, M., Green, C., Goodenough, D. A. and Kistler, J. (1995). Changes in lens connexin expression lead to increased gap junctional voltage dependence and conductance. *Am. J. Physiol.* **269**, C590-C600.
- Donaldson, P., Kistler, J. and Mathias, R. T. (2001). Molecular solutions to mammalian lens transparency. *News Physiol. Sci.* **16**, 118-123.
- Ebihara, L. and Steiner, E. (1993). Properties of a nonjunctional current expressed from a rat connexin46 cDNA in *Xenopus* oocytes. *J. Gen. Physiol.* **102**, 59-74.
- Evans, W. H. and Martin, P. E. (2002). Gap junctions: structure and function (Review). *Mol. Membr. Biol.* **19**, 121-136.
- Gao, J., Sun, X., Martinez-Wittinghan, F. J., Gong, X., White, T. W. and Mathias, R. T. (2004). Connections between connexins, calcium, and cataracts in the lens. *J. Gen. Physiol.* **124**, 289-300.
- Gerido, D. A. and White, T. W. (2004). Connexin disorders of the ear, skin, and lens. *Biochim. Biophys. Acta* **1662**, 159-170.
- Gerido, D. A., DeRosa, A. M., Richard, G. and White, T. W. (2007). Aberrant hemichannel properties of Cx26 mutations causing skin disease and deafness. *Am. J. Physiol.* **293**, C337-C345.
- Goldberg, G. S., Lampe, P. D. and Nicholson, B. J. (1999). Selective transfer of endogenous metabolites through gap junctions composed of different connexins. *Nat. Cell Biol.* **1**, 457-459.
- Gong, X., Li, E., Klier, G., Huang, Q., Wu, Y., Lei, H., Kumar, N. M., Horwitz, J. and Gilula, N. B. (1997). Disruption of alpha3 connexin gene leads to proteolysis and cataractogenesis in mice. *Cell* **91**, 833-843.
- Gong, X., Cheng, C. and Xia, C. H. (2007). Connexins in lens development and cataractogenesis. *J. Membr. Biol.* DOI:10.1007/s00232-007-9003-0.
- Gray, J., Loster, J., Soewarto, D., Fuchs, H., Meyer, B., Reis, A., Wolf, E., Balling, R. and Hrabe de Angelis, M. (2001). Characterization of a mutation in the lens-specific MP70 encoding gene of the mouse leading to a dominant cataract. *Exp. Eye Res.* **73**, 867-876.
- Harris, A. L. (2001). Emerging issues of connexin channels: biophysics fills the gap. *Q. Rev. Biophys.* **34**, 325-472.
- Jiang, J. X. and Gu, S. (2005). Gap junction- and hemichannel-independent actions of connexins. *Biochim. Biophys. Acta* **1711**, 208-214.
- Le, A. C. and Musil, L. S. (2001). A novel role for FGF and extracellular signal-regulated kinase in gap junction-mediated intercellular communication in the lens. *J. Cell Biol.* **154**, 197-216.
- Mackay, D., Ionides, A., Kibar, Z., Rouleau, G., Berry, V., Moore, A., Shiels, A. and Bhattacharya, S. (1999). Connexin46 mutations in autosomal dominant congenital cataract. *Am. J. Hum. Genet.* **64**, 1357-1364.
- Makowski, L., Caspar, D. L., Phillips, W. C. and Goodenough, D. A. (1977). Gap junction structures. II. Analysis of the x-ray diffraction data. *J. Cell Biol.* **74**, 629-645.
- Martinez-Wittinghan, F. J., Sellitto, C., Li, L., Gong, X., Brink, P. R., Mathias, R. T. and White, T. W. (2003). Dominant cataracts result from incongruous mixing of wild-type lens connexins. *J. Cell Biol.* **161**, 969-978.
- Mathias, R. T., Rae, J. L. and Baldo, G. J. (1997). Physiological properties of the normal lens. *Physiol. Rev.* **77**, 21-50.
- Milks, L. C., Kumar, N. M., Houghten, R., Unwin, N. and Gilula, N. B. (1988). Topology of the 32-kd liver gap junction protein determined by site-directed antibody localizations. *EMBO J.* **7**, 2967-2975.
- Niessen, H., Harz, H., Bedner, P., Kramer, K. and Willecke, K. (2000). Selective permeability of different connexin channels to the second messenger inositol 1,4,5-trisphosphate. *J. Cell Sci.* **113**, 1365-1372.
- Paul, D. L., Ebihara, L., Takemoto, L. J., Swenson, K. I. and Goodenough, D. A. (1991). Connexin46, a novel lens gap junction protein, induces voltage-gated currents in nonjunctional plasma membrane of *Xenopus* oocytes. *J. Cell Biol.* **115**, 1077-1089.
- Rong, P., Wang, X., Niesman, I., Wu, Y., Benedetti, L. E., Dunia, I., Levy, E. and Gong, X. (2002). Disruption of Gja8 (alpha8 connexin) in mice leads to microphthalmia associated with retardation of lens growth and lens fiber maturation. *Development* **129**, 167-174.
- Runge, P. E., Hawes, N. L., Heckenlively, J. R., Langley, S. H. and Roderick, T. H. (1992). Autosomal dominant mouse cataract (Lop-10). Consistent differences of expression in heterozygotes. *Invest. Ophthalmol. Vis. Sci.* **33**, 3202-3208.
- Shiels, A., Mackay, D., Ionides, A., Berry, V., Moore, A. and Bhattacharya, S. (1998). A missense mutation in the human connexin50 gene (GJA8) underlies autosomal dominant "zonular pulverulent" cataract, on chromosome 1q. *Am. J. Hum. Genet.* **62**, 526-532.
- Spray, D. C., Harris, A. L. and Bennett, M. V. (1981). Equilibrium properties of a voltage-dependent junctional conductance. *J. Gen. Physiol.* **77**, 77-93.
- Steele, E. C., Jr, Lyon, M. F., Favor, J., Guillot, P. V., Boyd, Y. and Church, R. L. (1998). A mutation in the connexin 50 (Cx50) gene is a candidate for the No2 mouse cataract. *Curr. Eye Res.* **17**, 883-889.
- Valiunas, V., Beyer, E. C. and Brink, P. R. (2002). Cardiac gap junction channels show quantitative differences in selectivity. *Circ. Res.* **91**, 104-111.
- Veenstra, R. D. (1996). Size and selectivity of gap junction channels formed from different connexins. *J. Bioenerg. Biomembr.* **28**, 327-337.
- White, T. W. (2003). Nonredundant gap junction functions. *News Physiol. Sci.* **18**, 95-99.
- White, T. W. and Bruzzone, R. (1996). Multiple connexin proteins in single intercellular channels: connexin compatibility and functional consequences. *J. Bioenerg. Biomembr.* **28**, 339-350.
- White, T. W., Bruzzone, R., Goodenough, D. A. and Paul, D. L. (1992). Mouse Cx50, a functional member of the connexin family of gap junction proteins, is the lens fiber protein MP70. *Mol. Biol. Cell* **3**, 711-720.
- Willecke, K., Eiberger, J., Degen, J., Eckardt, D., Romualdi, A., Guldenagel, M., Deutsch, U. and Sohl, G. (2002). Structural and functional diversity of connexin genes in the mouse and human genome. *Biol. Chem.* **383**, 725-737.
- Xia, C. H., Cheung, D., DeRosa, A. M., Chang, B., Lo, W. K., White, T. W. and Gong, X. (2006a). Knock-in of alpha3 connexin prevents severe cataracts caused by an alpha8 point mutation. *J. Cell Sci.* **119**, 2138-2144.
- Xia, C. H., Liu, H., Cheung, D., Cheng, C., Wang, E., Du, X., Beutler, B., Lo, W. K. and Gong, X. (2006b). Diverse gap junctions modulate distinct mechanisms for fiber cell formation during lens development and cataractogenesis. *Development* **133**, 2033-2040.
- Xu, X. and Ebihara, L. (1999). Characterization of a mouse Cx50 mutation associated with the No2 mouse cataract. *Invest. Ophthalmol. Vis. Sci.* **40**, 1844-1850.